THREE-STAGE OPTIMIZATION METHOD FOR DISTRIBUTED ENERGY SYSTEM DESIGN UNDER UNCERTAINTY

by

Zhenyu WANG[a,b], Chu Peng XIAO[a,b], Hao LI[c*], Chaoyang XU[a,b], Jun ZHAO[c], Wenjun RUAN[d], and Song GUO[a,b]

[a] Nari Group Corporation/State Grid Electric Power Research Institute, Nanjing, China
[b] State Grid Electric Power Research Institute Wuhan Efficiency Evaluation Company Limited, Wuhan, China
[c] Key Laboratory of Efficient Utilization of Low and Medium Grade Energy (Tianjin University), Ministry of Education of China, Tianjin, China
[d] State Grid Jiangsu Electric Power Co., LTD. Nanjing, China

Original scientific paper
https://doi.org/10.2298/TSCI190521382W

Reasonable capacity configurations of distributed energy system are issues which need to be discussed. Determinate design without considering variations in energy load and energy prices can result in non-achievement of project targets during its service life. Therefore, a design method that takes into account uncertain factors takes precedence over other methods. In this paper, a three-stage optimization method is proposed to provide theoretical guidance on the optimization of combined cooling, heating, and power system configurations. The first two stages link the optimization of the operation strategy and equipment capacities simultaneously under current load and energy prices. The Monte-Carlo simulation is applied in the third stage to fully consider the effects of various possible scenarios, and the Tabu search algorithm was introduced for system optimization. The comprehensive benefits include energy consumption, economy, and emission level. These were taken into consideration in the objective function. Moreover, a detailed design process was presented to illustrate the application of the proposed method. In conclusion, the proposed method is not only suitable for the design of combined cooling, heating, and power system, but could easily extend to other energy system easily.

Key words: *uncertainty analysis, combined cooling, heating, and power system, three-stage optimization method, information entropy, planning*

Introduction

Uncertainty modeling and research in distributed energy systems (DES) has drawn a fair share of attention in recent years. The energy input, transformation, output, their relationship with each other, and the uncertainty of each part in the energy hub need to be further studied in the modeling process.

Economic considerations determine the ability of the DES to survive. However, it is difficult to provide a more precise estimation of the uncertainty in the actual operation during the design stage. At present, there are many kinds of programing models, but the chosen value of each uncertain parameter in the algorithm is usually on the basis of experience, which is the main reason that results in the actual economy deviate from the expected. In addition to the

* Corresponding author, e-mail: tju_lihao1992@163.com

uncertainty of renewable energy output and energy demand, it is imperative to make a more comprehensive consideration of energy carrier price uncertainty during the design stage.

The type of system known as combined cooling, heating, and power (CCHP) systems have become preferred in many different scenarios because of their qualities of being efficient and flexible, and their advantages of being clean and reliable. Because of the limitations to the possible configurations for such a system, it is difficult to balance the heating/cooling and power load demands on such a system when considering the applications independently. In order to optimize the CCHP system, Mancarella *et al.* [1] modeled a CCHP system with a combined gas-fired boiler and electric chiller by considering the real-time management of demand while the economy was optimized under the load demand for the different seasons. The energy migration analysis was also done for different energy shifting strategies. Li *et al.* [2] took economic, environmental, and energy saving rates as the different optimization objectives, and compared the configurations under different energy loads of the residential and office buildings. The comprehensive performance of office buildings was found to be superior due to the use of air conditioners and energy storage devices. Ren *et al.* [3] analyzed the performances of a solar energy system combined with fuel, cells in a DES in Japan with the goal of performing environmental, economic, and sensitivity analyses to optimize these parameters considering the effects of the carbon tax. Wu *et al.* [4] compared the economic, environmental, and energy saving rates of a CCHP system integrated with an auxiliary gas-fired boiler under five typical climates and four different types of buildings in Japan. Wang *et al.* [5, 6] analyzed the sensitivity of the gas and electricity prices on the systems' operation strategy.

The equipment capacity must be identified at the design stage, and the mode of operation should lead to an economic optimum. In the stage after the sensitivity analysis research, a multitude of uncertainties were taken into consideration for the design of the DES [7], including the instability of the renewable energy output caused by ambient conditions and the fluctuation of energy demand. Pang and O'Neill [8] optimized the configurations and control parameters of the gas-fired domestic hot water supply systems in commercial buildings by applying uncertainty and sensitivity analysis. The insufficient gas supply incident was also considered as the result of an uncertainty factor in the district energy system integrated with combined heat and power and wind power [9]. In addition, the flexible-stochastic programming method was a mature algorithm developed to reveal the effects of municipal uncertainty in energy planning [10, 11].

The uncertainties inherent in these systems need to be considered in the design stage to maintain the profitability of the projects in their operational lifetimes, while conventional systems design methodologies considering operational strategy treat energy demand as a deterministic series. In this paper, a methodology for DES design under uncertainty parameters is investigated. The methodology includes the modeling of optimal DES design, load modeling, definition of the probability distributions of the uncertain parameters, and uncertainty analysis using Monte-Carlo simulations (MSC). Finally, the system configurations of the DES need to be improved to accommodate the uncertainty in future operations.

Methodology for uncertainty investigation

The CCHP system model

A typical CCHP system assisted by a gas boiler and an electric chiller is shown in fig. 1. The electricity, heating and cooling energy flows are represented in green, red, and blue, respectively. In this section, a detailed model of the proposed optimization method will be introduced. The typical CCHP system running under the strategy of determining power generation by heat. A separate system is introduced as a comparison scheme to provide the basis for CCHP system optimization. In the separate system, the electricity, heating and cooling energy is supplied by the grid, a gas-fired boiler, and an electrical chiller. A detailed model of the system is presented in *Appendix A.1* supplementary material. As a case study for this paper, the design of a CCHP system for an office building with an area of 14400 m^2, is investigated. The purpose of our design is to meet the energy requirements of buildings, including power, heating and cooling load, under various conditions.

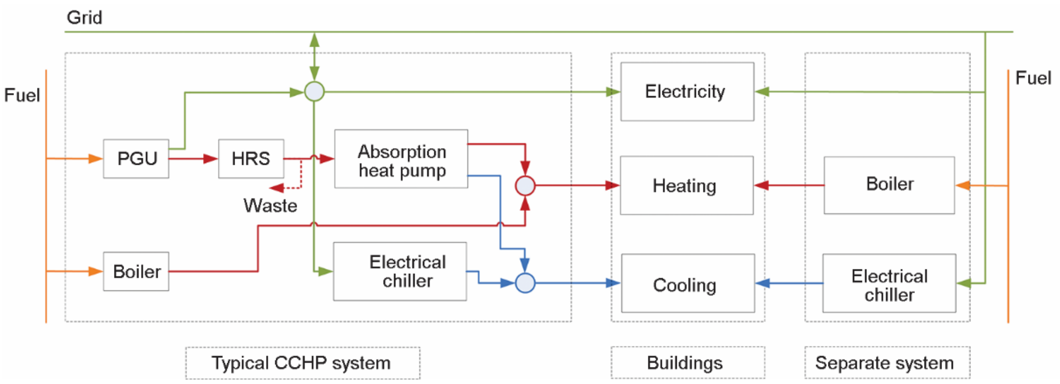

Figure 1. The structure of a typical CCHP system and a separate system; PGU – power generation unit, HRS – heat recovery system

Energy load

A detailed model of the energy load is presented in *Appendix A.2* supplementary material.

Quantification of uncertainty

Energy carrier prices

In the traditional deterministic design, the usual values of natural gas prices are the current prices at the design stage. However, they are not static throughout the life cycle. The economic cost/benefit outcome of the project is largely determined by the energy carrier prices, which vary according to import prices, exploitation technology, government policy, and even the international energy markets and are difficult to predict accurately at the design stage. Thus, it is reasonable to treat natural gas prices as uncertain parameters in the design. A uniform distribution, U (= 2-3.5) [12] was considered.

Considering the time-of-use grid electricity price, not only would the prices change with the access of renewable power to the grid, so would the peaks and valleys of the periods of the renewable energy use. With the increase of renewable energy production, the real-time electricity price could be a critical measure of demand response in electricity markets. In this paper, a stochastic increase or decrease was added to current electricity prices. A uniform distribution, U (= 0.3-0.5) was considered.

Emission factors

The emission factor of natural gas is regarded as a constant value due to negligible variations in the fuel's carbon content. However, the emission factor of grid electricity incorporates the purchase cost from the grid under a carbon tax, as well as the feed-in tariff, and thus, influences the economics of the project. However, the emission factor of grid electricity is forecast to decrease because of the increasing use of RES to supply the grid. Nevertheless, the rate of descent is currently not determined. Hence, the emission factor of grid electricity needs to be treated as an uncertain parameter in the design stage. Based on the different ways of accounting for carbon emissions and the differences in the main power supply in different areas, the emission factors of grid electricity can vary greatly. Thus, to characterize the uncertainty of the emission factors of grid electricity, a uniform distribution, U (= 0.478-1.0416) kgCO_2/kWh was defined as the current range of emission factors according to the emission factors of grid all around China. An uncertain rate of descent was defined as an additional term to the current factors due to increasing use of RES, and the range of rate of descent is U (= 0-2%).

Meteorological parameters

For a specific region, the monthly mean temperature radiation remain at a relatively stable level, while the hourly meteorological parameters may change with the appearance of extremely cold or warm seasons. Therefore, the probability distribution models of meteorological parameters were established, generating random meteorological parameters according to the monthly mean data. The N [a, b] is a normal distribution with mean value, a, and standard deviation, b. The probability distribution models of ambient temperature and radiation are shown in tab. 1.

Table 1. The probability distribution models of ambient temperature and radiation

Uncertainty values	Base values	Distributions	Notes
Monthly mean ambient temperature	t_{o_monthly}	$t_{o\_\mathrm{monthly}} + N\,[0,2]$	[14]
Monthly mean daily horizontal radiation	G_{o_monthly}	$G_{o\_\mathrm{monthly}} + N\,[0,0.8]$	[14]

The hourly meteorological parameters were generated by adding random values onto the base values. The base values of the hourly meteorological parameters were exported from building load simulation software in the DeST [13]. The random hourly data was generated according to a normal distribution whose mean values are the differences of the base values and random values of monthly mean meteorological parameters, having a standard deviation of 0.5. The hourly meteorological parameters are no longer a set of certain values, but a range of possible values.

Indoor environmental parameters

Indoor set temperature: In the load simulation, the indoor set temperature is usually set at 26 °C in cooling season, and 20 °C in heating season. The indoor temperatures often deviate from the design temperatures due to personnel preferences in the actual operation, which causes the cooling or heating load to rise and fall. Therefore, the indoor set temperature was considered as following a triangular probability distribution, T [a, b, c], with lower limit a, upper limit c, and the likeliest value b.

Staff indoor rate: The staff indoor rate indicates the presence of people inside the room and number of people. The range of the staff indoor rate is [0,1], with the upper limit indicating that the room is at full capacity and the lower limit indicating that the room is empty. The lower the staff indoor rate, the lower is the load. A triangular probability distribution was used to demonstrate the uncertainty of the staff indoor rate. The number of persons in the room should be equal to the maximum number it is designed to hold to maximize the staff indoor rate.

Ventilation rate: This indicates the ratio of actual ventilation quantity to design value. Adjusting the ventilation time significantly influences the heating and cooling load and it is an uncertain parameter. Here, the ventilation rate is set as 1 and the ventilation quantity is set according to the national standard. It is described as a normal distribution with the parameters N [0,0.5].

Equipment demand coefficient influences power load and cooling load. The value was 0.9 in the certain parameter design. Other cases use the distribution N [0,0.5] to generate a random number to create a new equipment demand coefficient. The probability distributions of indoor environmental parameters are summarized in tab. 2.

Table 2. Probability distributions of indoor environmental parameters

Uncertainty parameters	Base value	Possibility distribution
Indoor set temperature	$t_{\mathrm{i\_heating}} = 20$ °C	$t_{\mathrm{i\_heating}} + T[18,20,24]$
	$t_{\mathrm{i\_cooling}} = 26$ °C	$t_{\mathrm{i\_cooling}} + T[22,26,28]$
Staff indoor rate	$\rho = 0.8$	$T[0.5,0.8,1]$ (workday) $T[0.1,0.2,0.3]$ (weekend)
ventilation rate	$\Phi = 1$	$\Phi + N[0,0.5]$
Equipment demand coefficient	$W = 0.9$	$W + N[0,0.5]$

Optimization method

In the optimization, the configurations of a DES are relevant to the system operation strategies. The output of a CCHP system must match the load instantaneously and the operation strategies greatly affect the running configurations throughout the year. However, once the configurations are identified, the strategies will be restricted to optimizing the performance of the equipment relative to its capacity. In this paper, a three-stage optimization method considering uncertainty was proposed to optimize the operation strategy and capacities simultaneously. The flow of the three-stage optimization method is shown in fig. 2.

The first stage is to optimize the operation strategy. From an operating perspective, if heat-to-electric ratio deviates from the performance curve, the cogeneration will produce large amounts of excess heat/power, or there will be a need to supply certain amounts of heat/power irrespective of whether the following electric load and following thermal load strategies are used. Thus, the optimization target is to find a point with minimal excess energy while simultaneously achieving maximal benefits for energy consumption, economy and emission levels. The partial-load ratio of the GPU and the output of the facilities are chosen as the independent variables in this stage of optimization.

$$\begin{gathered}\max Z[r_{\mathrm{ice,i}},\quad X(i),\quad Q_{\mathrm{ac,i}},\quad R_{\mathrm{ac,i}},\quad Q_{\mathrm{gb,i}},\quad R_{\mathrm{ec.i}}]\\ Z = \omega_1 OCS_i + \omega_2 PES_i + \omega_3 CER_i \\ \omega_1 + \omega_2 + \omega_3 = 1\end{gathered} \tag{1}$$

For each moment, the comprehensive performance of the CCHP system including the operation cost saving rate, the primary energy saving rate and the carbon reduction rate could be expressed:

$$OCS_{\mathrm{i}} = \frac{OC_{\mathrm{SP,i}} - OC_{\mathrm{DES,i}}}{OC_{\mathrm{SP,i}}} \tag{2}$$

$$PES_{\mathrm{i}} = \frac{PE_{\mathrm{SP,i}} - PE_{\mathrm{DES,i}}}{PE_{\mathrm{SP,i}}} \tag{3}$$

$$CER_{\mathrm{i}} = \frac{CE_{\mathrm{SP,i}} - CE_{\mathrm{DES,i}}}{CE_{\mathrm{SP,i}}} \tag{4}$$

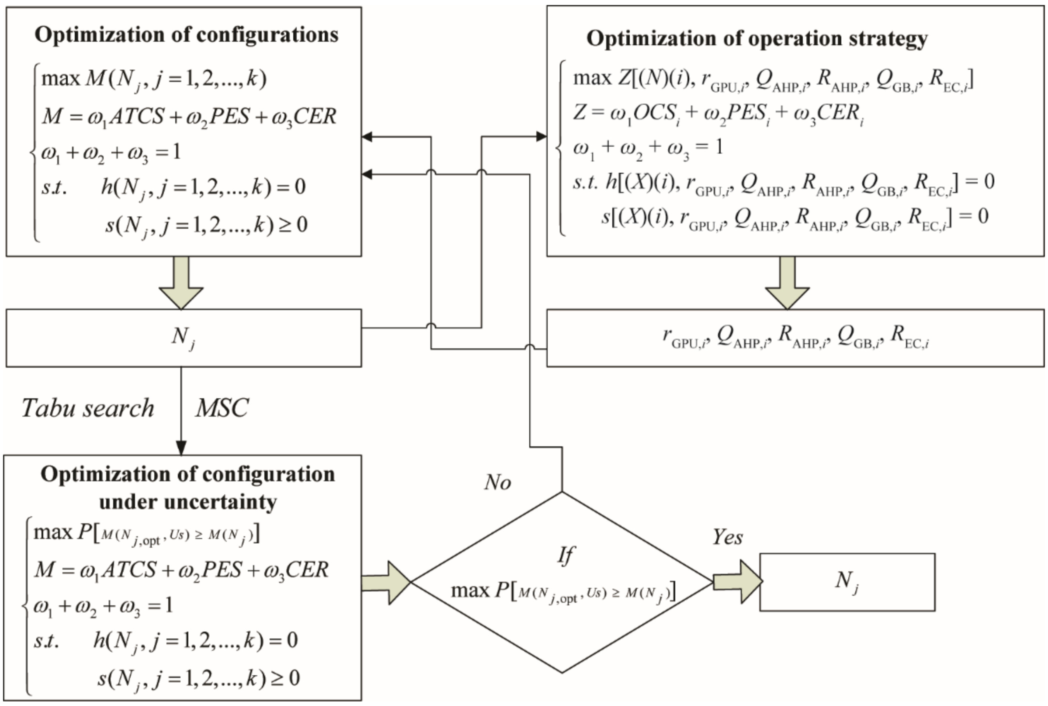

Figure 2. Three-stage optimization methods of CCHP system by considering uncertainty

The second stage is to optimize the configurations that aim to maximize the comprehensive benefits of the DES in its service life. Therefore, the independent variable of the design optimization stage is the capacity of each device. As described in the operation strategy optimization, the energy, economic, and emission reduction benefits of the system are also taken into consideration and the multi-objective decision-making method is adopted to seek the optimal configurations of the system. The objective function of system design optimization is:

$$\begin{gathered} \max M(N_j, \quad j=1,2,...,k) \\ M = \omega_1 ATCS + \omega_2 PES + \omega_3 CER \\ \omega_1 + \omega_2 + \omega_3 = 1 \end{gathered} \tag{5}$$

The optimization method of DES proposed in this paper organically links the operation strategy and configurations optimization. Using the optimal configurations achieved in the second stage, the MCS is applied in the third stage to fully consider the possibilities of various scenarios. The objective of the MCS is to obtain the results under various sets of conditions and attach a probability that the system will achieve certain levels of performance [15, 16]. A detailed discussion of MCS and its application to DES is shown in [14, 17]. The failure probability is proposed to describe the degree of deviation from the design points. In this stage, the probability distributions of the uncertainties are the input parameters in each simulation and the results differ for each set of conditions. The optimization objective is:

$$\max P[M(N_{j,\text{opt}}, Us) \geq M(N_j)] \tag{6}$$

where $M(N_j)$ refers to the comprehensive benefit of the determinate design during the first two stages, $N_{j,\text{opt}}$ is the final optimal configurations, and $M(N_{j,\text{opt}}, Us)$ refers to the comprehensive benefit of the final optimal configurations under uncertainty in each simulation in the MCS. The optimization objective is that the feasible probability reaches its maximum value. We consider the result of one simulation as a failure if the $M(N_{j,\text{opt}}, Us) < M(N_j)$. In this paper, 1000 MCS were conducted.

Case study

Energy demand

A high-tech industrial zone consisting mainly of office buildings in Tianjin, China was taken as a planning case. The heating, cooling, and power load characteristics are shown in fig. 3. By considering the uncertainties of the energy demand, the hourly heating, cooling, and power loads are not a series of determinate parameters but ranges in a probability space. The heating season runs from November 15 to March 15, and the cooling season runs from June 1 to September 31. There is no heating or cooling load at other times of the year. The power load does not fluctuate significantly all year round, but is relatively lower on weekends because of the low staff indoor rate.

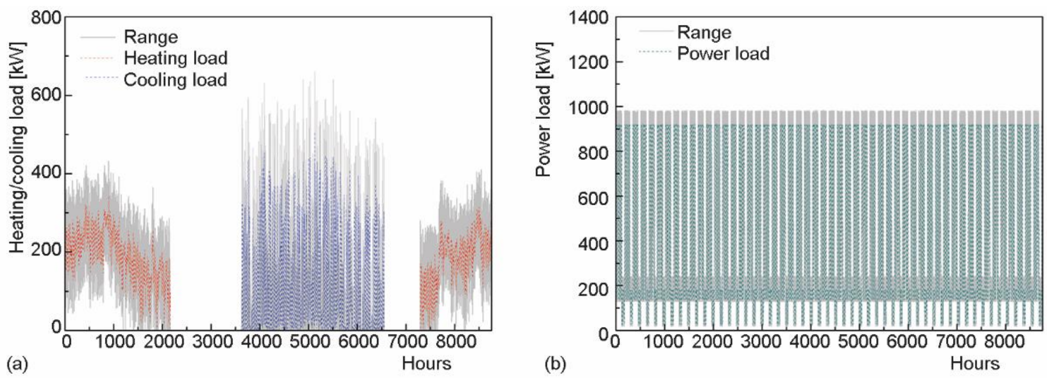

Figure 3. Heating, cooling and power load under uncertainty; (a) heating and cooling load and (b) power load

Determinate design

The determinate design involves the first two-stages in the three-stage design method. For the purposes of engineering applications, the capacity of a facility is usually a multiple of 10 kW. In addition, minimizing the initial investment required for the system was a con straint added at this stage, with the intention to offset the fact that creating a larger capacity CCHP results in a higher comprehensive benefit. The optimal configuration results in the GPU at 1000 kW, AHP at 980 kW, EC at 0 kW, and GB at 0 kW. The comprehensive performance of the CCHP is 0.14. With this configuration, the results illustrated that the GPU and AHP could meet the determinate (without uncertainty applied) heating and cooling load without the assisted EC and GB under the current energy prices. Insufficient electricity was supplied from power grid. Conventional design stops here, so it could not be confirmed whether the built-up CCHP system could realize the comprehensive benefit when the load and energy prices vary. In the next section, the design configurations will be improved to adapt to the uncertainty.

Sensitivity analysis

The results of MCS were divided into the failure group and the feasible group. The feasible group includes simulations wherein the comprehensive performance of the CCHP is better than the design value. Information entropy was applied to identify which factor had the most remarkable influence on the comprehensive performance of the CCHP. Refer to the detailed discussions about the information entropy in the sensitivity analysis for further discussion [18]. The information entropy of each uncertain parameter was shown in fig. 4. According to the results, the price of natural gas, c_{gas}, is the most influential factor. The effect of the feed-in tariff, c_{sale}, and the price of electricity purchased from the grid, c_{peak}, c_{valley}, and c_{flat}, are essentially the same because of the linear association between them. The differences among the electricity use peak, flat, and valley price, c_{peak}, c_{valley}, and c_{flat}, are not significant because there is no consideration of heat storage. By contrast, the ambient temperature variations, $\Delta t_{\mathrm{winter}}$, $\Delta t_{\mathrm{summer}}$, show less influence because of the good load regulation abilities of the CCHP.

Design improvement

The probability density function (PDF) according to the results of MCS was illustrated in fig. 5. The probability that the comprehensive benefits are higher than 0.14 is 54.7%, which means that there is a 45.3% chance that the economy of the project is failing to live up to expectations under these uncertainty considerations. The optimization objective of this stage is to maximize the feasible zone, which also indicates the design configurations have strong adaptability.

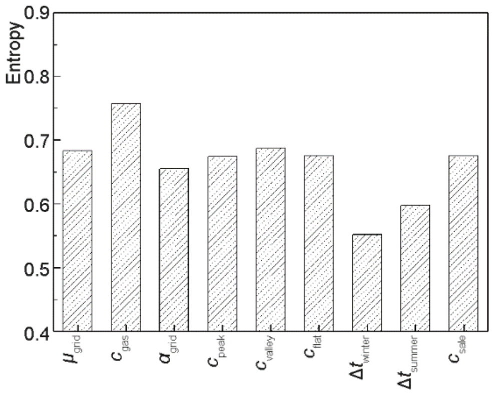

Figure 4. The information entropy of each uncertainty parameter

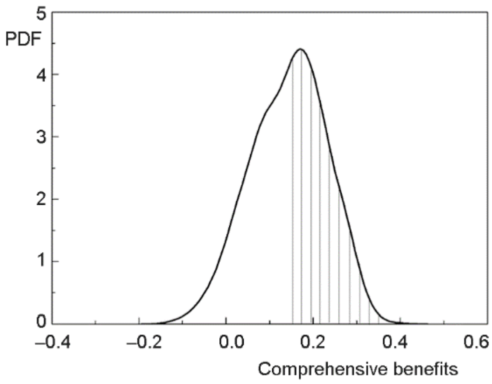

Figure 5. Distribution of comprehensive benefits according to MCS

The natural gas price is the most influential factor; hence, the capacities of GPU first need to be resized on the basis of the sensitivity analysis. The Tabu search (TS) algorithm [19] was applied to optimize the configurations. In order to avoid the calculation results falling into local optimal, the TS is a optimization algorithm that guides a local heuristic search to explore the solution space beyond local optimum. The interval of the optimization is listed in tab. 3. The results of the third stage optimization give the GPU at 800 kW, AHP at 840 kW, EC at 240 kW, and GB at 80 kW. The probability that the comprehensive benefits are higher than the 0.14 is 87.2%, and the failure probability drops down to 12.8%.

Table 3. The optimization interval of the equipment

Equipment	Units	Optimization interval
GPU	kW_e	[0, 2000]
AHP	kW_h	Depend on GPU
EC	kW_e	[0,700]
GB	kW_h	[0, 500]

Before the three-stage optimization method was proposed, a global search using MCS was operated, which consumed a great deal of computing resources and time. One thousand samples were selected in the MCS. As the number of samples increases, the computing time required increases exponentially. In order to facilitate solving it under uncertain conditions, the first two stages could be regarded as the preprocessing methods of variable optimization.

The sets of optimization intervals of the equipment in the third stage concern both the results of determinate design and the maximum of the energy demand. According to multiple trials, the final optimization result is close to the determinate design result. Thus, the optimization intervals could be shortened to improve the search rate.

Results and discussion

Table 4 lists the comparison of the two-stage and three-stage design configurations. Compared to the results of the two-stage design, the capacity of GPU decreases and the capacities of EC and GB increase using the three-stage design. The capacity of AHP depends on the capacity of GPU. Because the effects of the fluctuation of the gas price are larger than that of buying electricity from the grid, decreasing the capacity of GPU protects against the risk of higher gas prices. The objective of increasing the capacities of EC and GB is to meet the cooling and heating load requirements and to make up for the lack of GPU. In addition, the initial investments of EC and GB are lower than that of GPU system.

Table 4. Comparison of the configurations between two-stage design and three-stage design

Configurations	Two-stage design	Three-stage design
GPU	1000 [kW_e]	800 [kW_e]
AHP	980 [kW_h]	840 [kW_h]
EC	0 [kW_e]	240 [kW_e]
GB	0 [kW_h]	80 [kW_h]

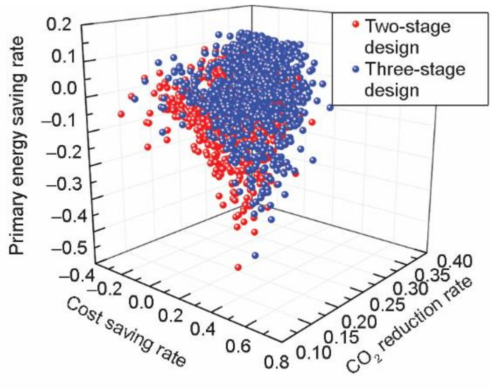

Figure 6. Comparison of the performances between two-stage design and three-stage design

In order to illustrate the improvement of the three-stage design in comparison to the two-stage design, the uncertainty of the output performances with variable parameters to simulate real conditions was reflected in the results shown in fig. 6. The comprehensive benefits gained from the results of the three-stage design are drastically improved compared to the two-stage design. While this improvement does not mean that it is advantageous under all conditions, it could ensure that the design indices are met under most conditions. The two-stage design method is just an optimization of the design under a single working condition, but it could not by itself satisfy a situation where the operating parameters deviate from the design conditions.

Conclusions

At present, the configurations of DES are designed according to the deterministically derived energy demand and current energy prices, which always leads to the operations in practice deviating from the design. In order to maintain highly competitive performance throughout the service life of the system, the uncertain parameters need to be considered in the design stage. In this paper, a three-stage optimization method for CCHP design under uncertain energy demand and energy prices was proposed. The first two stages tightly link the optimization of system design and operation strategies, and the third stage uses MCS to take into account the influences of uncertain parameters.

A CCHP system design case was conducted to exhibit the flow of the three-stage design methodology. Information entropy is applied to quantify the uncertainty and the significant level thresholds of each uncertain parameter. The results illustrate that the natural gas price has the most remarkable influence on the comprehensive performance of the CCHP. The result of the deterministic design (two-stage design) gives GPU at 1000 kW, AHP at 980 kW, EC at 0 kW, and GB at 0 kW. The optimization for the CCHP system under uncertain load and energy carrier prices gives the output of GPU at 800 kW, AHP at 840 kW, EC at 240 kW, and GB at 80 kW. The configurations could minimize the failure probability to 12.8%, which results in a 32.5% reduction *vs.* the deterministic design.

Acknowledgment

This work was supported by State Grid Science and Technology Project "Research and Development on Key Technology of Universal Energy Flow Model Based Regional Multi-energy System".

Nomenclature

ATCS – annual total cost savings rate
CE – CO_2 emissions [kg]
CER – CO_2 reduction rate
E – power generation/consumption, [kW]
F – gas consumption, [m^3h^{-1}]
G – radiation intensity, [Wm^{-2}]
IC – investment cost, [CNY]
LHV – low heat value, [kJm^{-3}]
N – installed capacity, [kW]
OC – operating cost, [CNY]
OCS – operation cost saving rate
PES – primary energy saving rate

Q – heating output, [kW]
Q_{re} – recovered waste heat from GPU, [kW]
r – part-load ratio
R – cooling output, [kW]

Greek symbols

α – primary consumption factor
μ – coefficient of carbon emissions [kghm^{-3}]
η_{e0} – rated power efficiency of GPU
η_{h0} – rated heating power efficiency of GPU
η_e – power efficiency of GPU
η_h – heating power efficiency of GPU

Subscript

GPU – gas-fired combined power unit
AHP – absorption heat pump
EC – electric chiller
GB – gas-fired boiler
grid – power grid
sa – sale

References

[1] Pierluigi Mancarella, G. C., Real-Time Demand Response from Energy Shifting in Distributed Multi-generation, *IEEE TRANSACTIONS ON SMART GRID*, *4* (2013), 4, pp. 1928-1938
[2] Li, L., *et al.*, Optimization and Analysis of CCHP System Based on Energy Loads Coupling of Residential and Office Buildings, *Applied Energy*, *136* (2014), Dec., pp. 206-216
[3] Ren, H., *et al.*, Multi-Objective Optimization for the Operation of Distributed Energy Systems Considering Economic and Environmental Aspects, *Applied Energy*, *87* (2010), 12, pp. 3642-3651
[4] Wu, Q., *et al.*, Multi-Criteria Assessment of Combined Cooling, Heating and Power Systems Located in Different Regions in Japan, *Applied Thermal Engineering*, *73* (2014), 1, pp. 660-670
[5] Wang, J., *et al.*, Sensitivity Analysis of Optimal Model on Building Cooling Heating and Power System, *Applied Energy*, *88* (2011), 12, pp. 5143-5152
[6] Wang, J. J., *et al.*, Optimization of Capacity and Operation for CCHP System by Genetic Algorithm, *Applied Energy*, *87* (2010), 4, pp. 1325-1335
[7] Mavromatidis, G., *et al.*, Uncertainty and Global Sensitivity Analysis for the Optimal Design of Distributed Energy Systems, *Applied Energy*, *214* (2018), Mar., pp. 219-238
[8] Pang, Z., O'Neill, Z., Uncertainty Quantification and Sensitivity Analysis of the Domestic Hot Water Usage in Hotels, *Applied Energy*, *232* (2018), Dec., pp. 424-442
[9] Fu, X., *et al.*, Failure Probability Estimation of the Gas Supply using a Data-Driven Model in an Integrated Energy System, *Applied Energy*, *232* (2018), Dec., pp. 704-714
[10] Lv, J., *et al.*, Planning Energy-Water Nexus System under Multiple Uncertainties – A Case Study of Hebei Province, *Applied Energy*, *229* (2018), Nov., pp. 389-403
[11] Yu, L., Li, Y. P., A Flexible-Possibilistic Stochastic Programming Method for Planning Municipal-Scale Energy System Through Introducing Renewable Energies and Electric Vehicles, *Journal of Cleaner Production*, *207* (2019), Jan., pp. 772-787
[12] *** http://data.stats.gov.cn/
[13] Yan, D., *et al.*, DeST – An Integrated Building Simulation Toolkit Part I: Fundamentals, *Building Simulation*, *1* (2008), 2, pp. 95-110
[14] Domínguez-Muñoz, F., *et al.*, Design of Solar Thermal Systems under Uncertainty, *Energy and Buildings*, *47*. (2012), Apr., pp. 474-484
[15] Rout, A., *et al.*, Risk Modeling of Domestic Solar Water Heater using Monte Carlo Simulation for East-Coastal Region of India, *Energy*, *145* (2018), Feb., pp. 548-556
[16] Olaru, M., *et al.*, Monte Carlo Method Application for Environmental Risks Impact Assessment in Investment Projects, *Procedia – Social and Behavioral Sciences*, *109* (2014), pp. 940-943
[17] Chauhan, A., Saini, R. P., Techno-Economic Optimization Based Approach for Energy Management of a Stand-Alone Integrated Renewable Energy System for Remote Areas of India, *Energy*, *94* (2016), Jan., pp. 138-156
[18] Fu, X., *et al.*, Uncertainty Analysis of an Integrated Energy System Based on Information Theory, *Energy*, *122* (2017), Mar., pp. 649-662
[19] Glover, F., Tabu Search, in: *Encyclopedia of Operations Research and Management Science*, (Ed., Editor Editors), Springer, Boston, Mass., USA, 2001, pp. 821-827

Appendix A. Supplementary material

CCHP system model

Gas-fired combined power unit (GPU)

As the core equipment of natural gas distributed energy system, the main parameters of the gas-fired combined power unit including the quantity of power generation, waste heat and gas consumption. The environment temperature has a little influence on the performance of gas fired combined power unit (GPU). Its rated efficiency varies with the installed capacity, which could be expressed [4]:

$$\eta_{e0} = 0.3513 + 1.15\cdot 10^{-4} N_{GPU} - 5\cdot 10^{-8} N_{GPU}^2 + 8\cdot 10^{-12} N_{GPU}^3 \tag{A1}$$

$$\eta_{h0} = 0.5646 - 2.27\cdot 10^{-4} N_{GPU} + 1\cdot 10^{-7} N_{GPU}^2 - 2\cdot 10^{-11} N_{GPU}^3 \tag{A2}$$

While the efficiency of GPU during actual operation varies with the part-load ratio, which could be expressed:

$$\eta_e = \eta_{e0}(0.0113 + 2.9801 r_{GPU} - 2.4726 r_{GPU}^2 + 0.4812 r_{GPU}^3) \tag{A3}$$

$$\eta_h = \eta_{h0}(1.5853 - 2.1247 r_{GPU} + 2.8870 r_{GPU}^2 - 1.3476 r_{GPU}^3) \tag{A4}$$

As a result, the quantity of power generation, waste heat and gas consumption could be expressed:

$$E_{GPU} = N_{GPU} r_{GPU} \tag{A5}$$

$$Q_{re} = \eta_h \frac{N_{GPU}}{\eta_e} \tag{A6}$$

$$F_{GPU} = 3600 \frac{\dfrac{E_{GPU}}{\eta_e}}{LHV} \tag{A7}$$

The CO_2 emissions related to the gas consumption, which could be calculated by:

$$CE_{GPU} = \mu_{GPU} F_{GPU} \tag{A8}$$

$$PE_{GPU} = \alpha_{gas} F_{GPU} \tag{A9}$$

The constraint is added to impose operational constraints on the GPU by considering the scope of power generation:

$$E_{GPU\_min} \le E_{GPU} \le E_{GPU\_max} \tag{A10}$$

In addition, the initial investment of GPU including purchase expense of internal combustion engine and heat recovery system, grid construction fee, waste disposal fee and installation fee and tax, the mathematical relationship between unit capacity investment cost and installed capacity could be fitted by the data given in [12]:

$$IC_{GPU} = 19756 + 3.6386 N_{GPU} - 4.2689\cdot 10^{-4} N_{GPU}^2 + 1.6704\cdot 10^{-8} N_{GPU}^3 \tag{A11}$$

Absorption heat pump

In the CCHP system, the absorption heat pump is driven by the high temperature flue gas waste heat to supply cooling in summer and heating in winter. The heating and cooling output of absorption heat pump (AHP) could be represented as the rated capacity of AHP and the recovered waste heat from PGU based on the data from Broad company:

$$Q_{\mathrm{AHP}} = N_{\mathrm{AHP}}(-0.1378 + 1.3467 r_{\mathrm{AHP}} - 0.2678 r_{\mathrm{AHP}}^2 - 0.0123 r_{\mathrm{AHP}}^3) \tag{A12}$$

$$R_{\mathrm{AHP}} = N_{\mathrm{AHP}}(-0.7179 + 5.0295 r_{\mathrm{AHP}} - 4.8430 r_{\mathrm{AHP}}^2 + 19.0876 r_{\mathrm{AHP}}^3) \tag{A13}$$

where the part-load ratio of the AHP could be expressed:

$$r_{\mathrm{ac}} = \frac{Q_{\mathrm{re}}}{N_{\mathrm{AHP}}} \tag{A14}$$

The constrain of the operation condition has to be within the minimum and maximum operation condition of AHP:

$$r_{\mathrm{AHP\_min}} \le r_{\mathrm{AHP}} \le r_{\mathrm{AHP\_max}} \tag{A15}$$

The initial investment of AHP could be deduced with rated capacity:

$$IC_{\mathrm{AHP}} = 72112 + 122.5 N_{\mathrm{AHP}} - 2.8589 \cdot 10^{-3} N_{\mathrm{AHP}}^3 \tag{A16}$$

Due to the AHP is driven by the recovered heat from gas engine units, therefore, here no longer double counting the CO_2 emissions.

Electric chiller

The electric chiller (EC) works as an auxiliary cooling supplier when the AHP could not meet the cooling load. The EC could increase the thermoelectric ratio in the energy system. In this research, with simplifying the mathematical model of EC, then the present performance of EC does not vary with the installed capacity and operating conditions, nor does the investment cost. The mathematical model could be expressed:

$$\begin{gathered} R_{\mathrm{EC}} = COP_{\mathrm{EC}} E_{\mathrm{EC}} \\ R_{\mathrm{EC\_min}} \le R_{\mathrm{EC}} \le R_{\mathrm{EC\_max}} \\ IC_{\mathrm{EC}} = c_{\mathrm{EC}} N_{\mathrm{EC}} \\ CE_{\mathrm{EC}} = \mu_{\mathrm{grid}} E_{\mathrm{grid}} \\ PE_{\mathrm{EC}} = \alpha_{\mathrm{grid}} F_{\mathrm{EC}} \end{gathered} \tag{A17}$$

Gas-fired boiler

The gas-fired boiler acts as an auxiliary heating source in the CCHP system, this paper assumes that the efficiency of gas-fired boiler (GB) does not vary with the installed capacity and operating conditions, nor does the investment cost. The mathematical model could be expressed:

$$
\begin{gathered}
Q_{\mathrm{GB}}=\frac{\eta_{\mathrm{GB}} F_{\mathrm{GB}} LHV}{3600} \\
F_{\mathrm{GB\_min}} \leq F_{\mathrm{GB}} \leq F_{\mathrm{GB\_max}} \\
IC_{\mathrm{GB}}=c_{\mathrm{GB}} N_{\mathrm{GB}} \\
CE_{\mathrm{GB}}=\mu_{\mathrm{gas}} F_{\mathrm{GB}} \\
PE_{\mathrm{GB}}=\alpha_{\mathrm{gas}} F_{\mathrm{GB}}
\end{gathered} \tag{A18}
$$

Paper submitted: May 21, 2019
Paper revised: August 13, 2019
Paper accepted: September 5, 2019